Research Square

Preprints are preliminary reports that have not undergone peer review.
They should not be considered conclusive, used to inform clinical practice,
or referenced by the media as validated information.

Organization of ice multiplication mechanisms among basic cloud types. Part II: Sensitivity tests

Akash Deshmukh

akash.deshmukh@univ-lille.fr

Université de Lille

Deepak Waman

Karlsruhe Institute of Technology

Ashok Kumar Gupta

Vanderbilt University

Vaughan Phillips

Lund University

Article

Keywords:

Posted Date: November 18th, 2026

DOI: https://doi.org/10.21203/rs.3.rs-11640438/v1

License: This work is licensed under a Creative Commons Attribution 4.0 International License.
Read Full License

Additional Declarations: No competing interests reported.

Organization of ice multiplication mechanisms among basic cloud types. Part II: Sensitivity tests

Akash Deshmukh[1*], Deepak Waman[2,3], Ashok Kumar Gupta[4], Vaughan Phillips[2*]

[1]University of Lille, CNRS, UMR 8518, Laboratoire d'Optique Atmospherique, Lille, France.

[2]Department of Physical Geography and Ecosystem Science, University of Lund, Lund, Sweden.

[3]Currently at Institute of Meteorology and Climate Research Troposphere Research, Karlsruhe Institute of Technology, Karlsruhe, Germany, Karlsruhe, Germany.

[4]Department of Earth and Environmental Sciences, Vanderbilt University, Nashville, Tennessee, USA.

*Corresponding author(s). E-mail(s): akash.deshmukh@univ-lille.fr; vaughan.phillips@mgeo.lu.se;

Abstract

Secondary ice production (SIP) governs ice concentrations and hence precipitation and electrification in clouds, yet how environment and microphysics control it remains unclear. In Part I, tracer-tagged simulations of four basic cloud types showed how cloud-base temperature and vertical velocity organize the SIP mechanisms. Here, sensitivity simulations of the same cases quantify how aerosols, cloud-base temperature and SIP shape cloud properties and storm electrification. In very warm-based convection, reducing cloud condensation nuclei raises ice concentrations in the lower mixed-phase region, whereas changing ice-nucleating particles has little effect because ice multiplication damps the response to either aerosol. Warming the cloud base raises ice concentrations in cold-based convection but lowers them in warm-based convection, where extra warm rain depletes the liquid sustaining collisional breakup. SIP buffers cloud ice against ice-nucleating particles: across 0.1 to 1000-fold changes, ice shifts by at most an order of magnitude with SIP but by up to three without it. Suppressing SIP cause the charge separation by 70-98% and reverses the polarity of graupel charging.

Keywords: ice multiplication, convection, cloud base, charge

1 Introduction

Mechanisms of secondary ice production (SIP) explain the discrepancy of several orders of magnitude between the concentrations of active ice nucleating particles (INPs), seen in *in-situ* observations of precipitating clouds [1–3], as noted in Part I. This discrepancy is known as 'ice enhancement'. Accurate prediction of ice concentrations therefore requires an understanding of SIP [4], because ice concentration regulates ice-phase precipitation [5], latent heating, the dynamics of vertical motion through cloud phase, and the radiative properties of clouds.

Changes in the loadings of cloud condensation nuclei (CCN) or INPs can alter the efficiency of ice multiplication processes [6, 7] and so modulate ice crystal concentrations. Polluted conditions may curb the HM process of rime splintering by reducing the number of large cloud droplets ($> 24\,\mu$m). A shift from maritime to continental aerosol can change precipitation from 'warm' to 'cold', depending on cloud-base temperature [5]. The associated shift in microphysical regime (Part I, Fig. 1 therein) would be expected to alter the relative activities of the SIP mechanisms, for instance by inhibiting raindrop-freezing fragmentation.

All known SIP involves precipitation somehow and is governed by the whole mixed-phase microphysical regime, consisting of the coexisting supercooled liquid and ice hydrometeors between 0 and about $-36\,^{\circ}$C, and the growth, riming, coalescence and freezing processes that link them. Consequently, ice multiplication is expected to depend strongly on environmental conditions, and evaluating ice enhancement must take account of the microphysical processes that reinforce or counteract it [5, 8]. Figure 1 shows the positive feedbacks driving ice multiplication. In the first, fragments from ice–ice collisions or rime splintering grow by diffusion and riming into ice precipitation that collides or rimes again, or are accreted by supercooled raindrops that freeze instantly into graupel, circumventing the lengthy period of vapor growth [9, 10] (Fig. 1a). In the second, fragments from supercooled raindrops freezing on collision with ice grow by vapor diffusion until large enough to intercept further raindrops [11, 12] (Fig. 1b). Both feedbacks are embedded in the wider web of coagulation, diffusional growth and particle initiation in mixed-phase clouds, and this interlinked web could be expected to give rise to synergy, whereby interrelated processes in a nonlinear microphysical system produce a larger combined effect than the sum of their isolated effects.

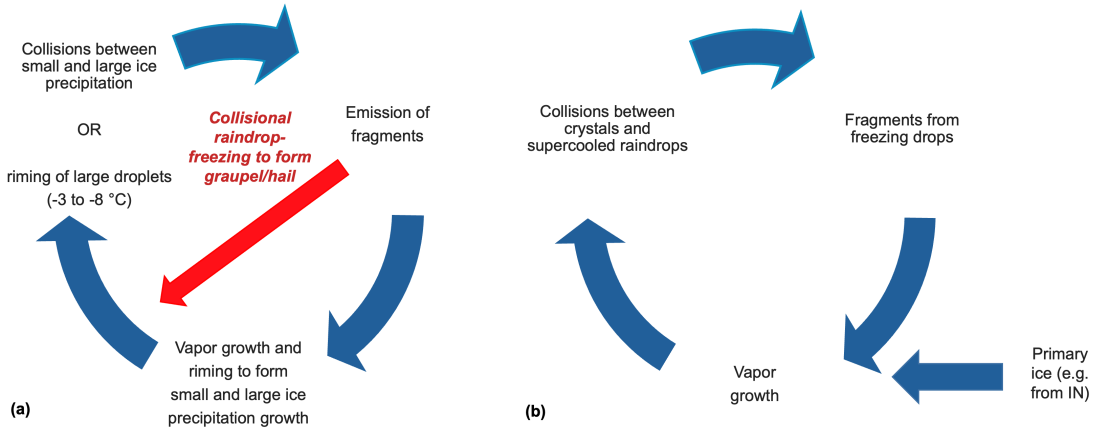


Fig. 1: Positive feedback loops of ice multiplication. (a) Fragments emitted from collisions between small and large ice precipitation, or from riming of large droplets (-3 to $-8\,^{\circ}$C), grow by vapor deposition and riming into small and large ice precipitation that collides or rimes again; collisional freezing of supercooled raindrops on the fragments (red arrow) forms graupel or hail directly, short-cutting the vapor-growth stage. (b) Fragments from supercooled raindrops freezing on collision with ice crystals grow by vapor deposition until large enough to collect further raindrops; primary ice from INPs (labelled IN) seeds the loop.

Among SIP mechanisms such synergy has been found, for example, between raindrop-freezing fragmentation and other fragmentation (Phillips et al.[11], their Fig. 7). The HM process and raindrop-freezing fragmentation tend to occur together because both require large cloud droplets ($> 24\,\mu$m for

rime splintering above about 20 μm for coalescence to form rain). Coexisting SIP processes may thus support one another through feedback loops that share ice fragments.

The environmental dependence of ice multiplication must also influence the electrification of deep convection. Lightning occurs preferentially over land rather than ocean, owing to the greater warmth of land in warm seasons and to polluted aerosol conditions [13, 14]. It arises from rebounding collisions between ice particles in supercooled cloud liquid, with differential sedimentation separating heavy and light ice particles of opposite polarity [15–18]. Phillips et al.[13, 14] showed that breakup in ice–ice collisions affects storm electrification, linking the intensity and polarity of charging, and the transport of charged hydrometeors, to the ice microphysics of the storm.

This Part II quantifies the role of environmental factors, particularly aerosol conditions and lower-tropospheric humidity in the balance among the SIP mechanisms and the synergies between them in the contrasting cloud types of Part I and elucidates the microphysical mechanisms of that linkage. Sensitivity simulations are performed with the Aerosol–Cloud model (AC) from the control simulations of the four observed cases typifying the basic cloud types, which were described and validated in Part I. The study does not encompass every cloud type in which SIP may be active (e.g., Arctic stratocumulus). The sensitivity tests are designed to answer three questions:

1. What effect does a change in aerosol loading (e.g., the land–ocean contrast) have for a given cloud type, does that effect differ between stratiform and convective clouds, and does a boost in INP loading intensify ice enhancement?
2. Does homogeneous ice nucleation aloft affect SIP in the mixed-phase region (0 to $-36\,^{\circ}$C) below, and does ice multiplication affect charge separation in cloud types generally, as found by Phillips et al.[13, 14] for one case of continental cold-based convection?
3. Is there synergy among the SIP mechanisms, as they share secondary ice fragments and precipitation among their positive feedbacks (Fig. 1), and does it depend on cloud type?

These experiments reveal contrasting aerosol sensitivities between warm-based and cold-based convection, and demonstrate the important role of secondary ice production in determining both ice concentrations and charge separation. The implications for cloud microphysics and electrification are discussed below.

2 Results

Part I analysed the control simulations of the four observed cases (ACAPEX, STEPS, MC3E and GOAmazon) that typify the basic cloud types; here those control runs are the baseline for the sensitivity tests described in Sec. 4.

2.1 Sensitivity tests for ice multiplication

Table 1 lists the sensitivity tests used to evaluate the individual roles of the SIP mechanisms and the synergy among them, in which each mechanism is switched off singly, kept on singly, or switched off in pairs (Sec. 4.2).

Table 1: Sensitivity simulations used to examine the individual roles of, and the synergy among, the ice multiplication mechanisms. Acronyms: Hallett–Mossop process (HM), raindrop-freezing fragmentation (RF), breakup in ice–ice collisions (BR) and sublimational breakup (SB).

Name of experimental case	**Description of the simulations**	
	Active SIP mechanisms	**Inactive SIP mechanisms**
Control run	All four mechanisms are active	None
No-SIP case	None	All four mechanisms
No-HM case	BR, RF and SB	HM
No-RF case	HM, BR and SB	RF
No-BR case	HM, RF and SB	BR
No-SB case	HM, BR and RF	SB
Only-HM case	HM	BR, RF and SB
Only-RF case	RF	HM, BR and SB
Only-BR case	BR	HM, RF and SB

Continued on next page

Name of experimental case	Description of the simulations	
	Active SIP mechanisms	Inactive SIP mechanisms
Only-SB case	SB	HM, BR and RF
No-HM-RF case	BR and SB	HM and RF
No-BR-SB case	HM and RF	BR and SB

2.2 Individual SIP processes

Figure 2 compares the ice concentrations from each SIP mechanism acting alone (the only-HM, only-RF, only-BR and only-SB runs), averaged over stratiform or convective cloud regions depending on the basic cloud-type typified by the case, with those of the no-SIP run. In the lower half of the mixed-phase region, each mechanism raises the ice concentration above the no-SIP value by about 0.5 to 2 orders of magnitude in all four cases. The cold-based STEPS case is the exception due to the lack of supercooled rain and the small cloud droplets practically prevent three of the four mechanisms, while breakup in ice–ice collisions alone boosts ice concentrations by about 3 orders of magnitude at those levels. In all four cases, inclusion of ice-ice collisional breakup with the only-BR run yields the highest ice concentrations in the mixed-phase region, out of the four single-mechanism runs.

Ice concentrations are larger by up to about an order of magnitude, in convective (STEPS, MC3E, GOAMAZON) than in stratiform (ACAPEX) cloud-types generally in the lower half of the mixed-phase region. This is because faster ascent supports more precipitation mass aloft and hence more ice multiplication (Figs. 2 and S1). This holds especially for the only-HM and only-RF runs in warmer-based cases, since convective ascent supplies both the supercooled cloud liquid and the rain that these two mechanisms require. However, above the $-25\,^{\circ}\mathrm{C}$ level in deep convection, the influence of any single mechanism relative to the no-SIP run becomes minimal (Figs. 2 and S2), because homogeneously nucleated ice at high concentration is downwelled into the upper half of the mixed-phase region in convective downdrafts and obscures the SIP processes signal.

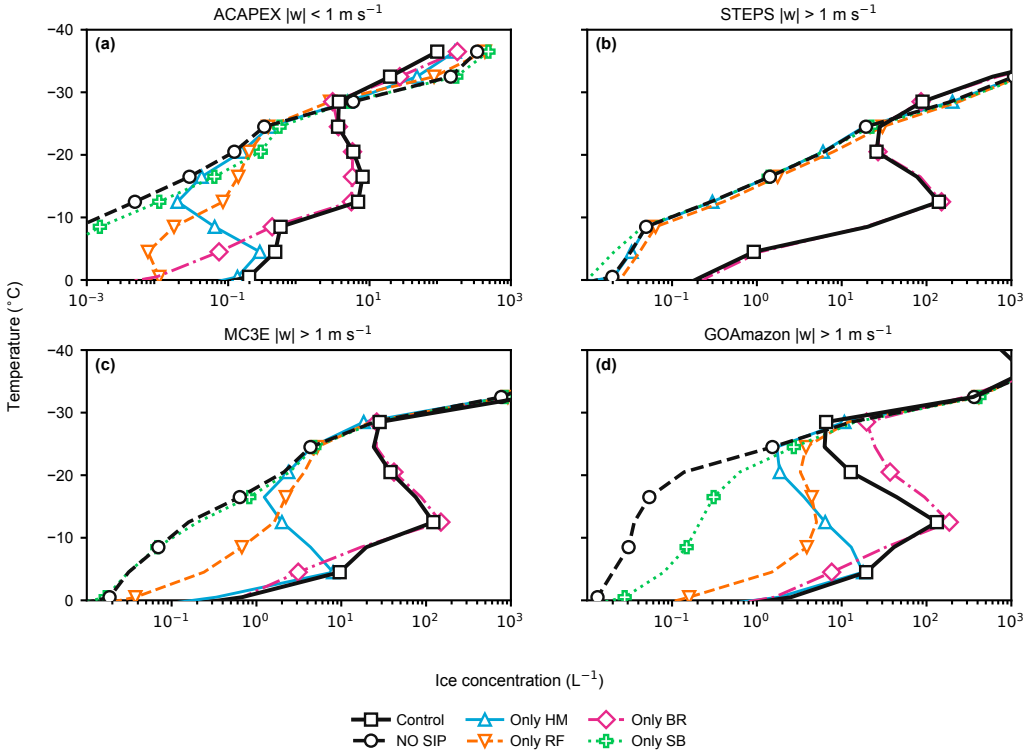


Fig. 2: Averaged vertical profiles of ice concentration for (a) the stratiform clouds of ACAPEX and the convective clouds of (b) STEPS, (c) MC3E and (d) GOAmazon, from the only-HM run (cyan upward triangles), only-RF run (orange downward triangles), only-BR run (magenta diamonds) and only-SB run (green crosses), together with the control run (black solid line, open squares) and the no-SIP run (black dashed line, open circles).

Removing breakup in ice–ice collisions (No-BR run) reduces ice concentrations below those of the control run by about 1 to 2.5 orders of magnitude in the stratiform and convective regions of all four cases (Fig. S3). There is a remarkable increase in ice concentration in the No-BR run of the warm-based case in the stratiform region of MC3E by up to an order of magnitude relative to the control run, due to a reduction in evaporation of cloud-liquid and increased homogeneous freezing aloft in the convective outflow(Fig. S3e,f). By contrast, the No-HM, No-RF and No-SB runs leave ice concentrations little altered in both regions of all cases. The exception is the No-HM run, in which ice concentrations fall by up to an order of magnitude in and below the HM generation region (-3 to $-8\,^{\circ}$C) of the slightly cold-based stratiform ACAPEX case (Fig. S3a), and by factors of about 3 and 2 in the convective ascent of the warm- and very warm-based cases, MC3E and GOAmazon (Fig. S3g,k).

2.2.1 Synergy of SIP mechanisms

Figure 3 reveals the synergy between pairs of SIP mechanisms. For each pair, the ice concentration from the run in which only that pair is active (for example the No-HM-RF run for BR and SB) is compared with the sum of the perturbations from the two mechanisms acting alone (the no-SIP profile plus the excess of only-BR over no-SIP plus the excess of only-SB over no-SIP). Where the combined profile lies above the sum for the pair is synergistic; where it lies below, then the pair is dyssynergistic, typically because the mechanisms compete for the same precursor species, such as supercooled cloud liquid or rain.

The HM process and raindrop-freezing fragmentation are strongly synergistic at warmer levels (around $-10\,^{\circ}$C) and dyssynergistic at colder levels (around $-25\,^{\circ}$C) in most cases. In the ACAPEX case typifying stratiform cloud, the combined effect exceeds the sum by a factor of about 1.5–2 near $-10\,^{\circ}$C, from sharing of splinters in their ice multiplication feedbacks, but falls below it near $-25\,^{\circ}$C (Figs. 3b), with similar behaviour in the embedded weak convection too (Fig. S2b). In the GOAmazon case of very warm-based convective cloud, the slight synergy at warmer levels in convective regions (factor of about 1.3–1.5) gives way to widespread dyssynergy at colder levels (Figs. 3k) (and in related stratiform regions too, in Fig. S2k). This dyssynergy is consistent with competition between both SIP processes for supercooled cloud droplets during riming and accretion. In MC3E for slightly warm-based convective clouds, again there is synergy at warmer levels (by up to a factor of about 1.3) and dyssynergy at colder levels in convective regions (Figs. 3h), (but some synergy at colder levels in stratiform regions Fig. S2h). The dyssynergy has a common cause: including either mechanism depletes supercooled cloud liquid during ascent and so reduces homogeneous freezing in the upper half of the mixed-phase region and including both depletes it further, so the combined profile falls below the summed one.

Breakup in ice–ice collisions and sublimational breakup exhibit the opposite vertical structure. At warmer levels, their combined effect is close to additive or weakly dyssynergistic, reflecting the limited activity of sublimational breakup there, whereas at colder levels (around $-25\,^{\circ}$C) in convective regions the pair becomes weakly synergistic, slightly exceeding the sum by a factor of about 1.1–1.3 in most cases (e.g., Fig. 3g). This is consistent with collisional breakup supplying a large population of ice particles that sublimational breakup then fragments further in subsaturated regions, with some of the fragments a reinforcing feedback. The very warm-based GOAmazon case is the exception, where prior depletion of cloud liquid makes the pair dyssynergistic (Fig. 3j).

The HM process and breakup in ice–ice collisions show no clear synergy in any case (Fig. 3, last column). In GOAmazon they are dyssynergistic below about $-10\,^{\circ}$C, with the combined effect only about half the sum (Fig. 3l), because both mechanisms draw on the same reservoir of supercooled cloud liquid and precipitation particles during riming and accretion, limiting the total enhancement when they operate together. The lack of synergy between both SIP processes is explicable in terms of the HM process being near the base of the mixed-phase region, while breakup in ice-ice collisions is concentrated in convective ascent aloft in the interior of the mixed-phase region.

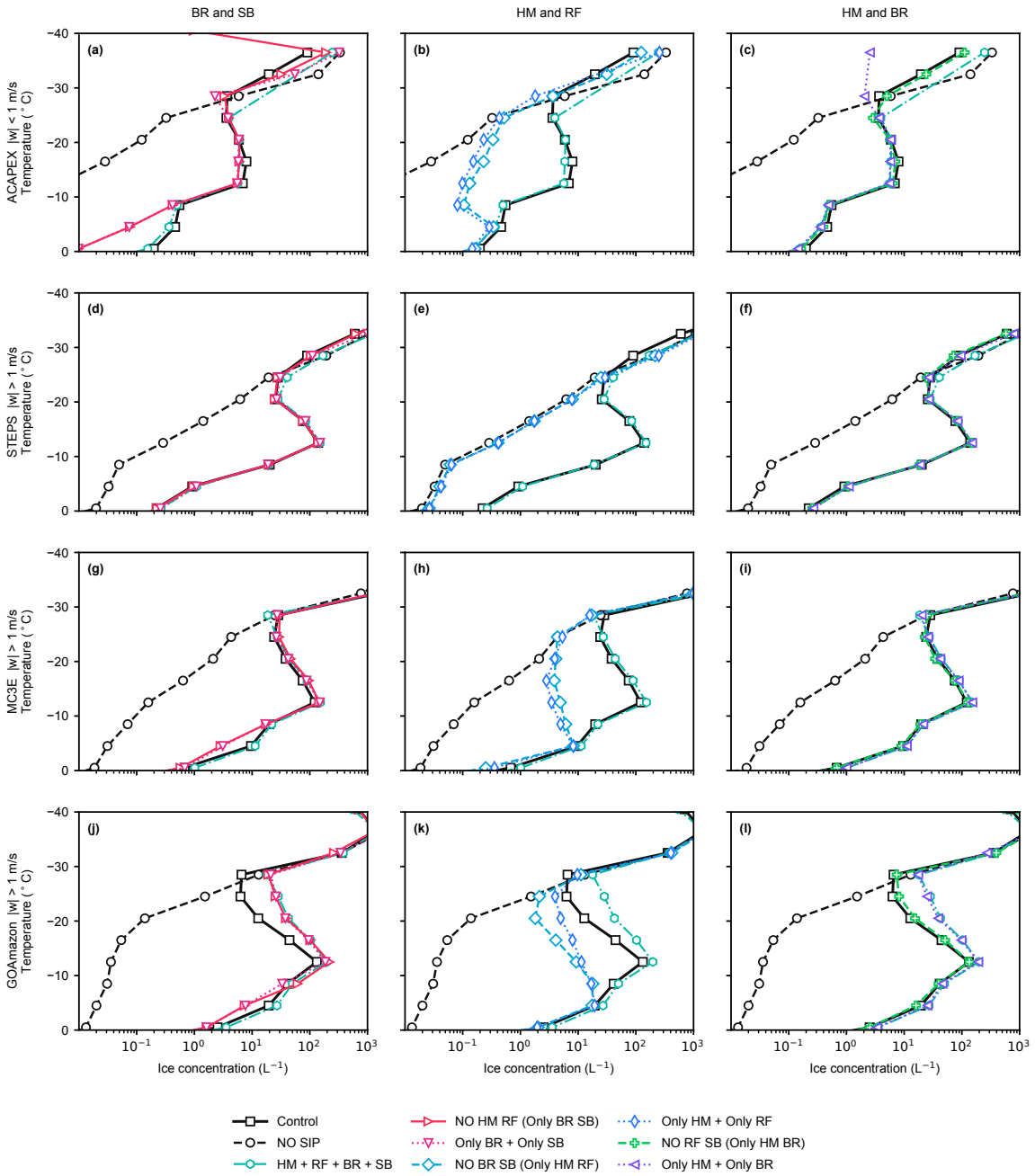


Fig. 3: Test for synergy between pairs of SIP mechanisms. Vertical profiles of ice concentration are shown for the stratiform regions of ACAPEX (a–c) and the convective regions of STEPS (d–f), MC3E (g–i) and GOAmazon (j–l); the column title names the pair tested. Each panel shows the control run (black open squares), the no-SIP run (black open circles), and the run with the pair switched off: No-HM-RF (red right triangles, solid line), No-BR-SB (blue diamonds, dashed line) or No-RF-SB (green crosses, dashed line). The dotted lines are the sums of the individual perturbations relative to the no-SIP run, that is, the no-SIP profile plus the excess of each single-mechanism run over it: only-HM + only-RF (blue diamonds), only-BR + only-SB (red downward triangles), only-HM + only-BR (purple left triangles), and all four mechanisms summed (only-HM + only-RF + only-BR + only-SB), (open hexagons). Synergy is indicated where the control run exceeds the corresponding sum.

Finally, with all four mechanisms active there is little or no net synergy at any subzero level, partly because breakup in ice-ice collisions is so much more prolific than the other mechanisms, so is boosted little by precipitation grown from their extra fragments. There is instead dyssynergy by up to a factor of about 2 in the upper half of the mixed-phase region of STEPS, MC3E and GOAmazon (open hexagons in Fig. 3), from the extra secondary ice depleting the cloud liquid otherwise available for homogeneous freezing.

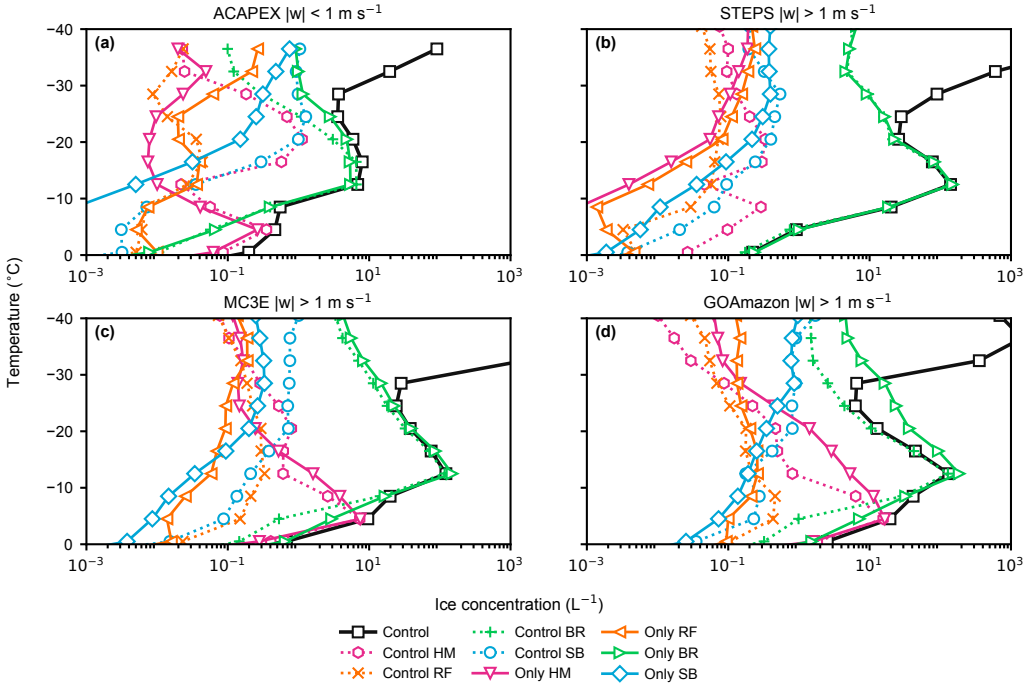


Fig. 4: Synergy of each SIP mechanism with all the others, from tagging tracers. Dotted lines with thin symbols show the tagged ice concentration from each mechanism in the control run: HM process (hexagrams), raindrop-freezing fragmentation (crosses), breakup in ice–ice collisions (plus signs) and sublimational breakup (circles); the total ice concentration of the control run is the black solid line with squares. Solid lines with the corresponding symbols show the total ice concentration from the run with only that mechanism active: only-HM (downward triangles), only-RF (left triangles), only-BR (right triangles) and only-SB (diamonds). Profiles are shown for the stratiform and convective regions of (a) ACAPEX, (b) STEPS, (c) MC3E and (d) GOAmazon.

Figure 4 compares the ice concentration of each SIP mechanism between the control run (its tagging tracer) and the total ice concentration of the run in which only that mechanism is active (only-HM, only-RF, only-BR and only-SB). The ratio of the two measures how much that mechanism is boosted (synergy) or suppressed (dyssynergy) by all the other ice multiplication acting around it, even where it is not the prevailing mechanism. In the stratiform clouds of ACAPEX, the HM component is boosted by up to about two orders of magnitude from the only-HM run to the control run (Fig. 4a), and the weak HM process in STEPS is boosted similarly. Sublimational breakup is boosted in the convective regions of all four cases at almost all levels, by a factor of 2 to 100 (Figs. 4 and S4). Raindrop-freezing fragmentation is boosted in the lower half of the mixed-phase region of convective cloud by up to a factor of about 10 in MC3E (0 to −25 °C) and 3 in GOAmazon (0 to −13 °C). Breakup in ice–ice collisions alone shows no synergy, or a dyssynergy, in all four cases, because it is so much more prolific than the other mechanisms that they cannot boost it, as noted above with all four mechanisms active.

Table 2: Summary of synergy among the SIP mechanisms from Figs. 3 and 4. Synergy, dyssynergy and no effect are denoted by ✓, × and –, respectively; a double checkmark denotes strong synergy and parentheses marginal synergy or dyssynergy. For GOAmazon, the lower entry in a split cell refers to the lower half of the mixed-phase region of convective clouds.

Case	**Individual SIP mechanisms**				**Synergy of total ice from all SIP**	**Paired SIP mechanisms**		
	Synergy of one SIP mechanism versus all other SIP mechanisms					Synergy of SIP pairs without other SIP mechanisms		
	HM	**RF**	**BR**	**SB**		**HM and RF**	**BR and SB**	**HM and BR**
ACAPEX	✓✓	✓	–	✓✓	–	✓✓	✓✓	✓

Case	Individual SIP mechanisms				Synergy of total ice from all SIP	Paired SIP mechanisms		
	Synergy of one SIP mechanism versus all other SIP mechanisms					Synergy of SIP pairs without other SIP mechanisms		
	HM	RF	BR	SB		HM and RF	BR and SB	HM and BR
STEPS	✓	✓	–	✓✓	×	(✓)	(✓)	×
MC3E	×	✓✓	–	✓✓	×	✓	(✓)	×
GOAmazon	×	✓✓	–	✓✓	×	× ✓	× ✓✓	×

In summary, Table 2 shows that every SIP mechanism except breakup in ice–ice collisions is strongly boosted by the other mechanisms acting around it, often by orders of magnitude, whereas collisional breakup is largely unaffected by them as it is much more prolific. Among pairs acting without the others, the HM process and raindrop-freezing fragmentation are strongly synergistic in ACAPEX and moderately so in the lower mixed-phase region of MC3E and GOAmazon, but dyssynergistic at colder levels through competition for supercooled cloud liquid. Collisional and sublimational breakup are generally synergistic, each supplying what the other fragments. The HM process and collisional breakup are dyssynergistic in most cases. With all four mechanisms active there is dyssynergy in most cases, from intensified depletion of supercooled cloud liquid and suppression of homogeneous freezing, except in the lower convective regions of GOAmazon. Synergy therefore depends on the combination of mechanisms, the cloud type and the favorable part of the mixed-phase region for each mechanism.

2.3 CCN sensitivity test with and without ice multiplication

Table 3 lists the sensitivity tests used to examine how SIP governs the response of ice concentrations to CCN and INP loadings (Sec. 4.3). In the CCN tests, the CCN concentration is increased or decreased by up to an order of magnitude in every case, with and without SIP.

Table 3: INP and CCN sensitivity simulations performed with AC. The factors applied to surface concentrations give the change in initial conditions relative to the control simulation (unity means no change) and are interpolated vertically from their surface values to unity in the upper troposphere [14].

Name of experimental case	SIP mechanisms	Factor for change in CCN/INP concentrations near the ground	
		CCN concentrations	INP concentrations
Control	Active	1	1
Low-CCN	Active	0.1 (0.2 for GOAmazon)	1
Low-CCN No-SIP	Inactive		
High-CCN	Active	10	1
High-CCN No-SIP	Inactive		
Low-dust	Active	1	0.1
Low-dust No-SIP	Inactive		
Slightly-high-dust	Active	1	10
Slightly-high-dust No-SIP	Inactive		
High-dust	Active	1	100
High-dust No-SIP	Inactive		
Extreme-dust	Active	1	1000
Extreme-dust No-SIP	Inactive		

Figure 5 (left panels) compares ice concentrations from the control run with those from the altered-CCN runs. In the lower half of the mixed-phase region there is little sensitivity in any of the four cases and the reduction of CCN produces no perceptible change. This is because, although CCN activation sets the concentration and mean size of the cloud droplets, breakup in ice–ice collisions drives the ice concentration to its maximum regardless. That maximum corresponds to the onset of subsaturation with respect to liquid and the total evaporation of supercooled cloud liquid [10],

irrespective of droplet concentration. By contrast, in the upper half of the mixed-phase region, ice from homogeneous freezing is downwelled from the −36 °C level, and its number concentration is set by the supercooled droplet concentration in the original convective ascent, so it does respond to CCN.

When the CCN test is repeated without secondary ice (Fig. 5, right panels), the sensitivity remains limited. In the lower half of the mixed-phase region of all cloud types, ice concentrations change by no more than a factor of about 2 in the High-CCN No-SIP and Low-CCN No-SIP runs relative to the No-SIP run; above the −10 °C level they increase by up to a factor of about 3 in the High-CCN No-SIP run.

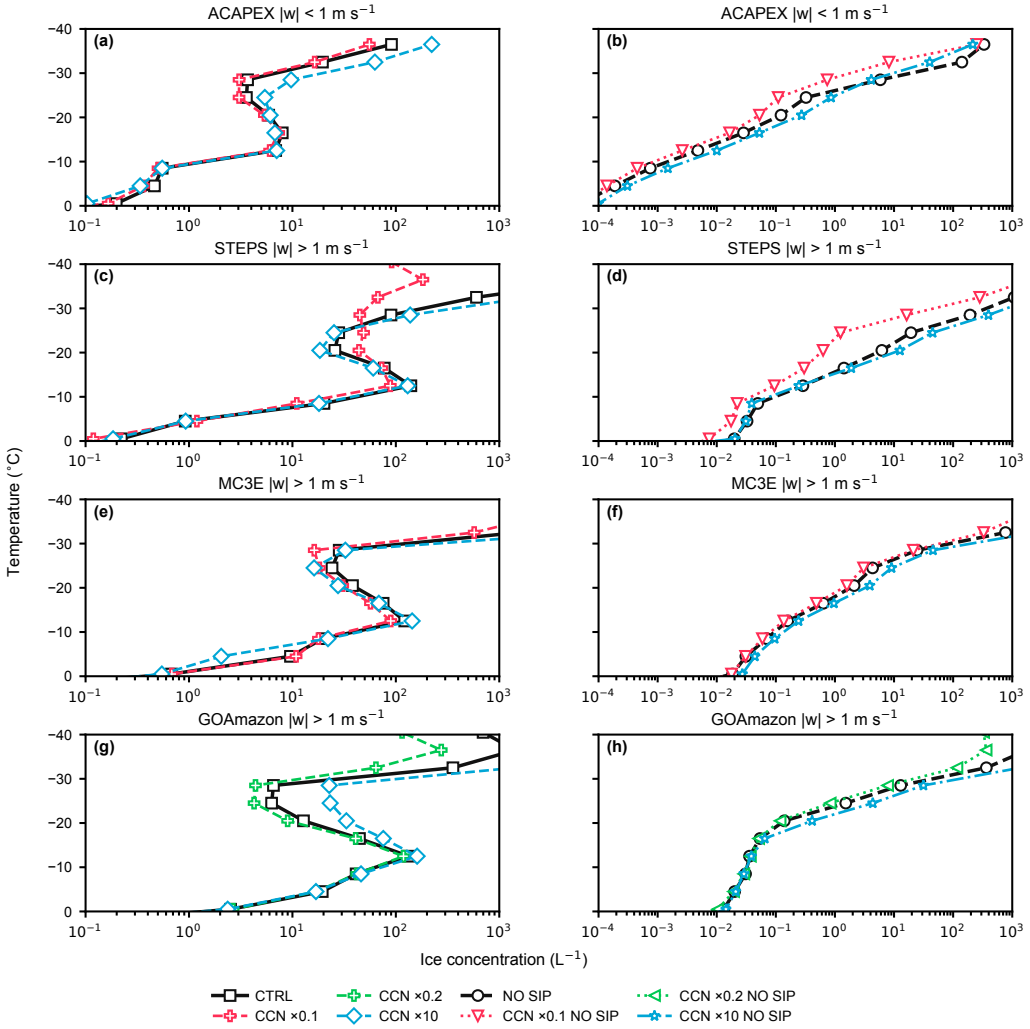


Fig. 5: Sensitivity of ice concentration to CCN with (left) and without (right) SIP, for the stratiform ACAPEX (a,b) and convective STEPS (c,d), MC3E (e,f) and GOAmazon (g,h) cloud systems. Left panels: control run (black squares), Low-CCN run with CCN ×0.1 (red plus signs) or ×0.2 for GOAmazon (green plus signs), and High-CCN run with CCN ×10 (open diamonds). Right panels: No-SIP run (open circles), Low-CCN No-SIP run (downward triangles, or left triangles for GOAmazon) and High-CCN No-SIP run (asterisks).

In summary, with SIP active, altering the CCN concentration slightly modifies the HM process but changes the other SIP processes by less than 30%. Without SIP mechanisms, total ice concentrations are again only weakly sensitive to CCN. Owing to the general weakness of this influence from CCN, there is little organisation by basic cloud-type.

2.4 INP sensitivity with and without ice multiplication

Figure 6 compares, among the various basic cloud-types, the impact on ice concentrations from altering environmental INP loading relative to the control run (Sec. 4.3; Table 3) with ice multiplication

active (left panels) and inactive (right panels). In the lower half of the mixed-phase region there is only slight sensitivity to the Low-dust (INP ×0.1) and Slightly-high-dust (INP ×10) conditions. This is because ice multiplication dominates the total ice concentration there and holds it close to the maximum at which supercooled cloud-liquid can still exist, which is generally needed for SIP [19, 20]. Once the ice concentration has risen to that maximum, the initial primary ice from INPs at the onset of glaciation no longer matters. By contrast, the High-dust (INP ×100) and Extreme-dust (INP ×1000) conditions raise ice concentrations by up to an order of magnitude in the lower half of the mixed-phase region, because the primary ice is then numerous enough to reach that maximum without SIP. In the Extreme-dust run the concentration of homogeneously nucleated ice in the upper half of the mixed-phase region falls by up to an order of magnitude, especially in the weaker ascent of ACAPEX (Fig. 6a), because the supply of supercooled cloud liquid in the ascent is depleted, leaving little for homogeneous freezing aloft.

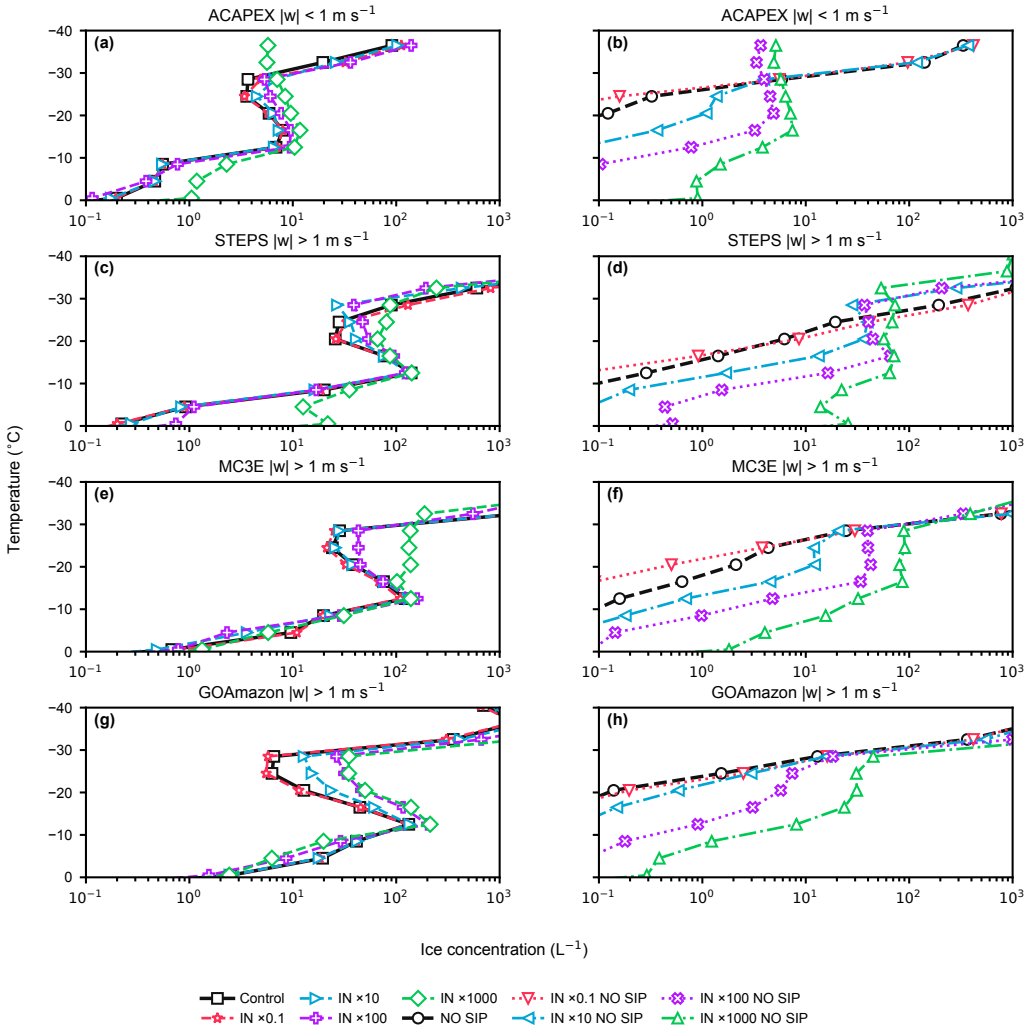


Fig. 6: Sensitivity of ice concentration to INP loading with (left) and without (right) SIP, averaged over the stratiform ACAPEX (a,b) and convective STEPS (c,d), MC3E (e,f) and GOAmazon (g,h) cloud regions. Left panels: control run (black open squares), Low-dust (INP ×0.1; red asterisks), Slightly-high-dust (INP ×10; blue right triangles), High-dust (INP ×100; magenta plus signs) and Extreme-dust (INP ×1000; green diamonds). Right panels: the corresponding No-SIP runs — No-SIP (black open circles), Low-dust No-SIP (red downward triangles), Slightly-high-dust No-SIP (blue left triangles), High-dust No-SIP (magenta crosses) and Extreme-dust No-SIP (green upward triangles).

Without ice multiplication (Fig. 6, right panels), ice concentrations are far more sensitive to INP loading which change from 0.5 to 3 orders of magnitude relative to the No-SIP run. Especially in the lower half of the mixed-phase region (Fig. 6b,d,f), where the INP-sensitive primary ice now sets the ice concentration at all levels warmer than −30 °C. As INP loading increases from Low-dust

to Extreme-dust that depletes of supercooled liquid water content (LWC) in the upper half of the mixed-phase region. Hence, the suppression of homogeneous freezing aloft varies much more without SIP than with it. This is especially so in the weaker ascent of the stratiform case (ACAPEX) at upper levels of the mixed-phase region due to depletion of supercooled cloud liquid at the highest INP loadings, preventing homogeneous freezing. SIP thus acts as a buffer against changes in INP.

Figure 7 gives the budget of ice particles produced over each entire simulation, split into primary ice, secondary ice and homogeneously nucleated ice, for the control and altered-INP runs. Secondary ice and homogeneous ice, which together determine the total ice and have little sensitivity to the change of INP concentrations in contrast with the primary ice..

In summary, the effect of altering environmental INP concentrations is suppressed similarly by ice multiplication in all four basic cloud types typified by ACAPEX, STEPS, MC3E and GOAmazon. The basic cloud-type has little role in this simulated linkage for INPs, although the stratiform case (ACAPEX) displays more sensitivity aloft at the highest IÄNP loadings.

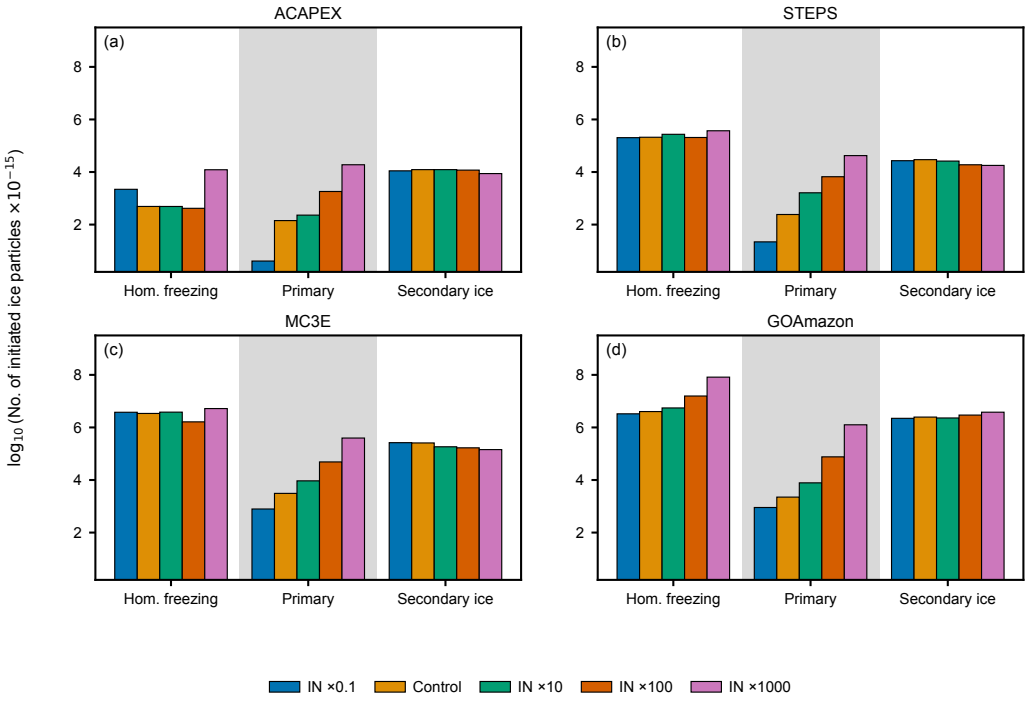


Fig. 7: Numbers of ice particles produced by homogeneous freezing of cloud liquid, primary ice nucleation and secondary ice production over the entire duration of the control, Low-dust (INP $\times 0.1$), Slightly-high-dust (INP $\times 10$), High-dust (INP $\times 100$) and Extreme-dust (INP $\times 1000$) runs, for ACAPEX, STEPS, MC3E and GOAmazon.

2.5 Homogeneous freezing effect on ice multiplication

Figure 8 compares averaged vertical profiles of ice concentration from the control, No-SIP and no-homogeneous-freezing runs. In all four cases, prohibiting homogeneous freezing of cloud liquid leaves ice concentrations unchanged below roughly the $-25\,^{\circ}$C level, that is over most of the mixed-phase region where SIP sets the total ice concentration. Above that level, the upper mixed-phase region is supplied mainly by downwelling of ice nucleated homogeneously near $-36\,^{\circ}$C. So, without homogeneous freezing the concentrations there are up to two orders of magnitude lower than in the control run. The influence runs the other way as well: the No-SIP run has more ice than the control, because ice multiplication in the convective updrafts depletes supercooled liquid and leaves less for homogeneous freezing. Overall, homogeneous freezing has no effect on ice multiplication at the levels where SIP dominates, whereas SIP does modulate homogeneous freezing. Again there is little dependency on the basic cloud-type for this impact.

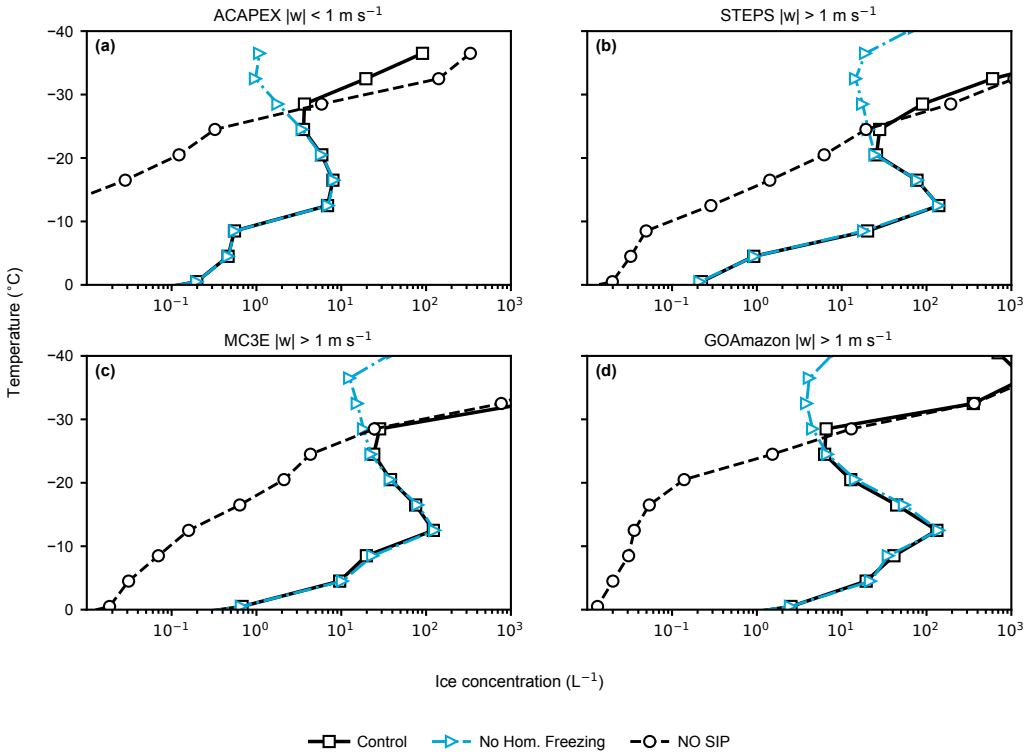


Fig. 8: Averaged vertical profiles of ice number concentration for the stratiform region of (a) ACAPEX and the convective regions of (b) STEPS, (c) MC3E and (d) GOAmazon, from the control run (open squares), the No-SIP run (open circles) and the no-homogeneous-freezing run (right triangles).

2.6 Contrasting effect on ice by lowering the cloud base of cold and warm-based convection

For STEPS and MC3E, the cloud base was lowered to a warmer level while the vertical-velocity statistics were held unchanged (Sec. 4.4). The purpose of the test is to isolate the effect on ice multiplication in convective regions from the shift in microphysical regime toward the warm-rain process.

Figure 9(a,b) displays the total ice concentration from the control, No-SIP and Low-cloud-base runs. In the STEPS case, lowering the cloud base raises the ice concentration above the control by about a factor of 2 between 0 and −25 °C and up to 3 between 0 and −10 °C, and the extra ice depletes the supercooled cloud liquid relative to the control (Fig. S5a). In the MC3E case the ice concentration instead falls by a similar factor of 2 to 3 between −10 and −30 °C, because the extra warm rain removes cloud liquid (Fig. S5b), so less graupel is produced by riming and breakup in ice–ice collisions weakens.

The tagged SIP components (Fig. 9c,d) show where the change comes from. In the originally cold-based case (STEPS), the contribution of the HM process rises by about 0.5 to 1 orders of magnitude, because the larger droplets in the HM region of the lowered-base cloud make rime splintering efficient, and the contributions of raindrop-freezing fragmentation and sublimational breakup each rise by about half an order of magnitude. In the originally warm-based case (MC3E) the corresponding contributions change by a factor of up to 3, increasing or decreasing according to the process.

In summary, the warmth of cloud-base in the control run determines how prone the cloud is to be influenced by warm rain as the base is lowered. Any such shift to warm rain by lowering the base then slightly reduces the intensity of SIP, which is largely graupel-dominated (e.g. in ice-ice collisional breakup).

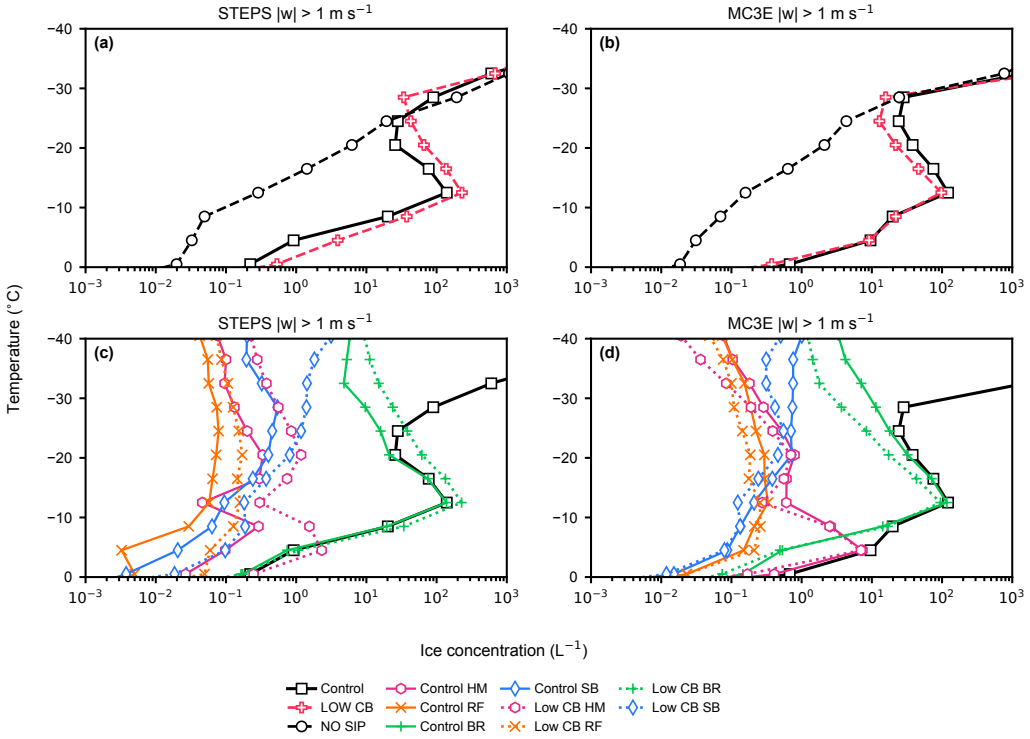


Fig. 9: Effect of lowering the cloud base in the convective regions of STEPS (a,c) and MC3E (b,d). (a,b) Vertical profiles of ice number concentration from the control run (open squares), the No-SIP run (open circles) and the Low-cloud-base run (plus signs, red dashed line). (c,d) Tagged components of the ice concentration from the HM process (hexagrams), raindrop-freezing fragmentation (crosses), breakup in ice–ice collisions (plus signs) and sublimational breakup (diamonds), from the control run (small symbols, solid lines) and the Low-cloud-base run (large symbols, dotted lines).

2.7 Charge separation and ice multiplication

The budget of all charge separated over each entire simulation shows a strong influence of ice multiplication on electrification (Fig. 10). Prohibiting all SIP is a test of causation only, not a realistic scenario, since ice multiplication is ubiquitous in deep convection.

In the ACAPEX control run of orographic cloud, the total charge separated in rebounding ice–ice collisions is very weak, about 21 kC, and 99.9% of the charge given to graupel is positive. Prohibiting SIP reduces the charge separated by a further 99.8% (Fig. 10a) and reverses the polarity of graupel charging, with only 30% of the charge on graupel positive (Fig. 10b).

The convective STEPS and MC3E thunderstorms respond similarly. Prohibiting SIP reduces the charge separated by about 60% and 90%, respectively, though the amount remaining is still enough to correspond to lightning. Both control runs give predominantly positive charging of graupel, as expected for a storm with normal charge structure and negative cloud-to-ground flashes [13]. Without SIP the graupel becomes predominantly negatively charged, because the supercooled liquid water content increases and shifts most of the charging into the negative regime of the LWC–temperature phase space (Phillips et al.[14], their Fig. 26), which would correspond to an inverted charge structure. Only with SIP included is the normal charge structure observed in STEPS reproduced.

In the very warm-based tropical GOAmazon case, the control run separates 2.1 MC of charge, 99% of it positive on graupel, again a normal charge structure. The supercooled LWC in the lower half of the mixed-phase region is weak, because 'warm' precipitation accretes it during the long ascent from cloud base to the high freezing level, so charging occurs mainly in the positive regime of the LWC–temperature phase space [14]. Prohibiting SIP suppresses the charge separated by about 98% and reverses the polarity of graupel charging, leaving only 10% positive, an inverted charge structure.

In all four cases, prohibiting homogeneous freezing of cloud liquid produces no appreciable change in the charge separated. In summary, both the intensity and the polarity of storm electrification are predicted to depend strongly on ice multiplication. While all basic cloud-types simulated show qualitatively similar reversal of the storm polarity when SIP is prohibited (from normal to inverted), the convective cases with colder bases display a greater degree of reversal.

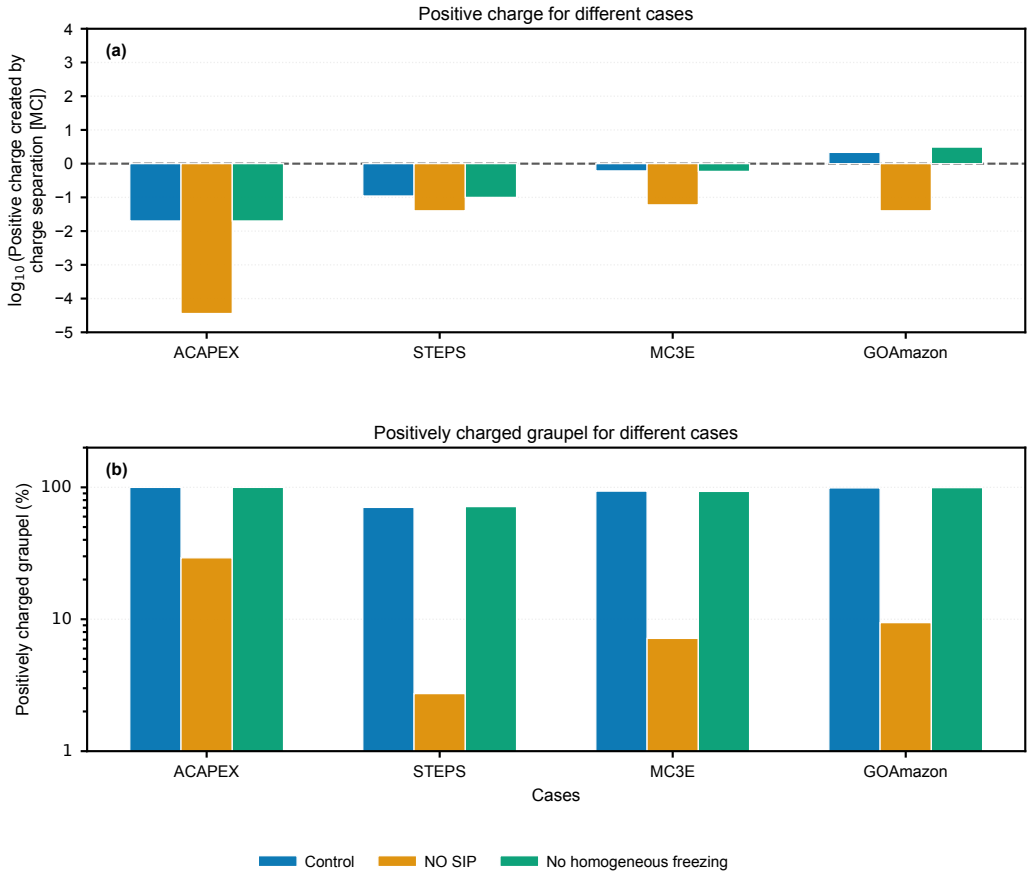


Fig. 10: Charge Separation in clouds. (a) Total charge separated by rebounding ice–ice collisions (MC) and (b) percentage of that charge that is positive on graupel, over the entire duration and domain of the control (blue), No-SIP (orange) and no-homogeneous-freezing runs, for ACAPEX, STEPS, MC3E and GOAmazon.

3 Discussion

Sensitivity simulations built on the control runs of the four basic cloud types that were described and validated in Part I. These simulations have been used to evaluate how secondary ice production responds to aerosol conditions, cloud-base temperature and homogeneous freezing, how the SIP mechanisms interact with one another and how ice multiplication governs storm electrification.

Each SIP mechanism acting alone raises ice concentrations by about 0.5 to 2 orders of magnitude over most of the mixed-phase region below the −25 °C level in ACAPEX, MC3E and GOAmazon, but has little effect above that level, where homogeneously frozen ice from higher levels aloft dominates. The cold-based convective (STEPS) case responds only to breakup in ice–ice collisions, because its cloud droplets are too small either for the HM process or for coalescence to supply rain for raindrop freezing, as expected from Part I. Conversely, removing collisional breakup from the control run reduces ice concentrations by 1 to 2.5 orders of magnitude, most of all in the cold-based convective case (STEPS) due to coldness of cloud base precluding other mechanisms. Removing any other single SIP mechanism changes little the overall ice concentrations, except for the HM process in and below its generation region (−3 to −8 °C) of the stratiform (ACAPEX) case and the two warmer-based convective cases.

The SIP mechanisms interact with each other. Every mechanism except collisional breakup is strongly boosted by the others acting around it and often by orders of magnitude. The leading mechanism of ice-ice collisional breakup is insensitive to all other SIP mechanisms. Among pairs acting in isolation, the HM process and raindrop-freezing fragmentation are strongly synergistic at warm levels in the stratiform case (ACAPEX), but dyssynergistic aloft through competition for supercooled cloud liquid. Also, collisional and sublimational breakup are generally synergistic. Overall, with all four mechanisms active the net effect is dyssynergistic from intensified depletion of cloud liquid and hence of homogeneous freezing.

Ice multiplication buffers the clouds against aerosol perturbations. With SIP active, changing CCN by an order of magnitude alters ice concentrations in the lower mixed-phase region by less than a factor of 2 in every case, because collisional breakup drives the ice concentration to the maximum compatible with supercooled liquid regardless of droplet number. Changing INP by an order of magnitude likewise leaves secondary and homogeneous ice almost unchanged; only increases of 2 to 3 orders of magnitude raise the total, while depleting the liquid available for homogeneous freezing in STEPS and MC3E. Without SIP, by contrast, ice concentrations respond to INP by 0.5 to 3 orders of magnitude.

A pivotal role for the organisation of the cloud-type/SIP linkage is the warmth of cloud-base and the related balance between both processes of precipitation production (warm rain process vs ice crystal process). This is elucidated by the sensitivity test involving warming of cloud-base while in-cloud ascent statistics remain unchanged. Lowering the cloud base to warmer levels is found to enhance ice concentrations by a factor of 2 to 3 in the convective region of cold-based STEPS, by activating the HM process and raindrop freezing. Also, reduction in ice concentration also seen for them by a similar factor in warm-based MC3E, where extra warm rain from invigorated coalescence (warm rain process) removes the cloud liquid needed for riming and collisional breakup. Prohibiting homogeneous freezing aloft has no effect on ice multiplication below $-25\,^{\circ}\mathrm{C}$ in any case.

Electrification depends strongly on ice multiplication. Prohibiting all SIP reduces the charge separated in rebounding ice–ice collisions by 60% (STEPS), 90% (MC3E), 98% (GOAmazon) and 99.8% (ACAPEX), and in every case reverses the polarity of graupel charging, from the predominantly positive charging of a normal charge structure to predominantly negative charging, with only 10% positive in GOAmazon, because the increased supercooled liquid shifts the charging into the negative regime of the LWC–temperature phase space. Prohibiting homogeneous freezing changes the charge separated by a negligible amount. Only with SIP is the observed normal charge structure of STEPS reproduced. Generally among convective cases, the colder the cloud-base the more extreme is the reversal of storm polarity predicted by prohibiting SIP, while the suppression of total charging is greater for warmer cloud bases.

In summary, regarding the organisational role of basic cloud-types, in stratiform (ACAPEX) and warm-based convective clouds (MC3E and GOAmazon), all SIP mechanisms enhance ice concentrations, whereas cold-based convection (STEPS) is mainly influenced by ice–ice collisional breakup. Ice–ice collisional breakup dominates SIP across all simulated cloud types, particularly in cold-based convective cloud. Strong positive synergy between the Hallett–Mossop (HM) process and raindrop-freezing fragmentation occurs in the simulated stratiform clouds, while convective clouds are predicted to exhibit positive synergy at lower levels and negative synergy aloft. Although individual SIP mechanisms generally display positive synergy when combined with other processes, their collective effects tend to produce negative synergy due to supercooled cloud-liquid depletion and suppression of homogeneous ice formation. Furthermore, SIP processes reduce the sensitivity of ice concentrations to CCN or INP variations in both stratiform and convective clouds, with lower CCN concentrations slightly favoring ice enhancement in the lower mixed-phase region. These results extend to a wider range of enviroronmental conditions, including the evaluation of the control runs of the same four cases in Part I and summarised by the conceptual schematic diagram (Deshmukh et al. 2026, their Figure 10). Part II assembled over the baseline of Part I to demonstrate ice multiplication against influencing factors to extend the understanding over changing conditions.

These conclusions rest on empirical SIP parameterizations whose laboratory basis is uneven. The existence of an efficient HM process has been questioned [21], although aircraft data remain consistent with it [2]. Also, sublimational breakup is formulated from only few of available laboratory studies [22] and Mode 2 of raindrop-freezing fragmentation (freezing on collision with ice) rests on a single study [23], whereas Mode 1 (freezing in free fall) derived from the observations [11]. Breakup in ice–ice collisions, the leading mechanism here, is the best constrained: field measurements of fragmentation of natural snow in Colorado and northern Sweden have yielded comparable formulations [24]. Since the environmental sensitivities found here hinge largely on collisional breakup, and since graupel–snow collisions are its most prolific source in these simulations [5, 25], because dense graupel carries high collision kinetic energy against fragile snow, graupel is pivotal for SIP. It is notable that the classic survey of hundreds of convective clouds by Harris-Hobbs and Cooper [2], interpreted at the time in terms of the HM process, found a strong dependence of secondary ice on graupel abundance aloft.

To conclude, three essential implications to follow from the findings of this 2-part study. Weather and climate models that represent SIP by the HM process alone omit the mechanism that sets both the ice concentration and its insensitivity to aerosol. So, they will overstate the aerosol sensitivity of mixed-phase clouds. The aerosol indirect effects of clouds are buffered by ice multiplication in these

simulations. Lightning parameterizations that do not represent SIP cannot reproduce the polarity of charging. And the sensitivities found here depend on the basic cloud type and all on cloud-base temperature above, so a single-case result should not be generalized across other cloud types.

4 Methods

4.1 Model and approach

The Aerosol–Cloud model (AC) is a cloud-resolving model developed by Phillips et al.[26] within the Weather Research and Forecasting (WRF) framework [27], with emulated bin microphysics and prognostic aerosol; its development is described by Phillips et al.[11, 13, 24–26, 28–30] and summarized in Part I. Four SIP mechanisms are represented: the HM process of rime splintering, breakup in ice–ice collisions, raindrop-freezing fragmentation and sublimational breakup. AC also contains an optional lightning component, a modified form of that of Barthe et al.[31], in which non-inductive charge separation in rebounding ice–ice collisions follows a modified formulation of the laboratory results of Takahashi [32, 33], with dependences on the sizes, relative fall speeds and bulk densities of the colliding particles; Phillips et al.[13] give details and a validation of predicted lightning for the STEPS storm. For computational efficiency the lightning discharge is not simulated here, but the charge separated in rebounding ice–ice collisions is budgeted over each simulation.

The four basic cloud types are represented by cases from the ARM Cloud Aerosol Precipitation Experiment (ACAPEX), the Severe Thunderstorm Electrification and Precipitation Study (STEPS), the Midlatitude Continental Convective Clouds Experiment (MC3E) and the Green Ocean Amazon (GOAmazon) campaign, whose control simulations were validated against coincident observations in Part I. Whereas Part I diagnosed the control runs with tagging tracers and budgets, the sensitivity tests here determine the hypothetical cloud properties in the absence of a target process, and so give its causal effect within the full web of competing and compensating processes. Each SIP mechanism is tracked by a tagging tracer for the number and mass of cloud ice it initiates, which is then carried passively through advection, diffusion, sedimentation and conversion to other species (a fragment that grows into snow remains tagged to its source) with the same sources and sinks as the total quantity. When a tagged particle itself initiates secondary ice, the new fragments are tagged to whichever mechanism produced them. Tracers do not influence the simulation.

4.2 Sensitivity tests for ice multiplication and synergy

For each cloud type, the SIP mechanisms are prohibited singly, retained singly, or prohibited in pairs (Table 1); the control run has all four active and the No-SIP run none. Synergy between two mechanisms A and B is assessed by comparing the ice concentration from the run in which only A and B are active with the sum of their separate perturbations, $N_{\mathrm{noSIP}} + (N_{\mathrm{onlyA}} - N_{\mathrm{noSIP}}) + (N_{\mathrm{onlyB}} - N_{\mathrm{noSIP}})$. The pair is synergistic where the combined run lies above this sum and dyssynergistic where it lies below. The synergy of one mechanism with all the others is assessed by comparing its tagged ice concentration in the control run with the total ice concentration of the run in which only that mechanism is active.

4.3 Sensitivity tests for CCN and INP

The environmental CCN or INP loading is scaled by a height-dependent factor, largest at the surface and decreasing linearly to unity in the upper troposphere [14], over a range spanning clean to polluted conditions and the land–ocean contrast (Table 3). Freshly emitted desert dust is represented by a factor of the same form that raises INP loading near the ground by up to three orders of magnitude; since AC treats droplet activation by solid aerosol (Part I), the added dust also alters CCN activity, although only the most extreme loadings increase droplet concentrations appreciably. To test whether SIP damps or amplifies the response to aerosol (Sec. 1), every CCN and INP test is repeated with all SIP prohibited in both the control and the perturbed run.

4.4 Other sensitivity tests

The no-homogeneous-freezing run prohibits homogeneous freezing of cloud droplets near $-36\,^{\circ}\mathrm{C}$ and of solute aerosol at colder temperatures. Comparison with the control run gives the effect of homogeneous freezing on ice multiplication, which might be expected because Heymsfield et al.[34] inferred from aircraft observations of a Florida convective core that homogeneously nucleated ice is downwelled in downdrafts and recirculated into the mixed-phase updraft.

The Low-cloud-base runs for STEPS and MC3E lower the cloud base by moistening the lower troposphere while holding the in-cloud statistics of ascent unchanged, following Gupta et al.[5], by means of a height-dependent temperature perturbation between cloud base and maximum cloud top. Holding ascent fixed isolates the microphysical effect of cloud-base temperature (in-cloud temperature,

cloud depth and adiabatic liquid water content, which bounds the actual LWC) from the thermodynamic effects that accompany a lower base in nature, where it can arise from either moistening (higher CAPE, faster ascent) or cooling (lower CAPE, slower ascent) of the lower troposphere [14]. The cloud base was warmed by 17 K in STEPS (from about 1 to 18 °C) and by 11 K in MC3E (from 17 to 28 °C), by raising surface relative humidity from 22% to 59% and from 48% to 99%, respectively, which raised CAPE from about 930 to 6000 J kg^{-1} in STEPS and from about 4570 to 12 000 J kg^{-1} in MC3E.

Supplementary information.

Acknowledgements. This work was guided by Vaughan Phillips and funded by an award (DE-SC0018932) to him from the Department of Energy (DoE), which aims at the modeling of secondary ice production in various cloud types. This research was also aided by an award to Akash Deshmukh, 'Endowments for the Natural Sciences, Medicine and Technology – Geoscience' from the Royal Physiographic Society of Lund. We thank Sachin Patade for his contribution in the model development.

- **Conflict of interest/Competing interests**
  The authors declare no competing interests.
- **Data availability**
  The STEPS sounding datasets are freely available from https://data.eol.ucar.edu/project/STEPS. The all data from ACAPEX is available on the given data portal - https://adc.arm.gov/discovery/results/iopShortName::aaf2015acapexaaf. The MC3E dataset are also freely available and can be obtained using https://ghrc.nsstc.nasa.gov/hydro/details/gpmcmmc3e. The observational datasets for the GOAmazon can be obtained from https://www.arm.gov/research/campaigns/amf2014goamazon.
- **Code availability**
  All the figures (including Supplementary Figures) are originally produced and plotted using open-source python libraries.
- **Author Contributions Statement**
  A.D. contributed to conceptualization, methodology, numerical simulations, formal analysis, investigation, manuscript drafting, review, and editing. D.W. and A.K.G. contributed to numerical simulations and manuscript review, with A.K.G. also contributing to editing. V.P. contributed to conceptualization, methodology, investigation, supervision, and manuscript review and editing. All authors reviewed and approved the final manuscript.

References

[1] Hobbs, P.V.: Ice multiplication in clouds. Journal of the Atmospheric Sciences **26**, 315–318 (1969) https://doi.org/10.1175/1520-0469(1969)026⟨0315:IMIC⟩2.0.CO;2

[2] Harris-Hobbs, R.L., Cooper, W.A.: Field evidence supporting quantitative predictions of secondary ice production rates. Journal of the Atmospheric Sciences **44**, 1071–1082 (1987) https://doi.org/10.1175/1520-0469(1987)044⟨1071:FESQPO⟩2.0.CO;2

[3] Taylor, J.W., *et al.*: Observations of cloud microphysics and ice formation during cope. Atmospheric Chemistry and Physics **16**, 799–826 (2016) https://doi.org/10.5194/acp-16-799-2016

[4] Field, P.R., *et al.*: Secondary ice production: Current state of the science and recommendations for the future. Meteorological Monographs **58**, 7–1720 (2017) https://doi.org/10.1175/AMSMONOGRAPHS-D-16-0014.1

[5] Gupta, A.K., Deshmukh, A., Waman, D., Patade, S., Jadav, A., Phillips, V.T., Bansemer, A., Martins, J.A., Gonçalves, F.L.: The microphysics of the warm-rain and ice crystal processes of precipitation in simulated continental convective storms. Communications Earth & Environment **4**(1), 226 (2023)

[6] Sullivan, S.C., Hoose, C., Nenes, A.: Investigating the contribution of secondary ice production to in-cloud ice crystal numbers. Journal of Geophysical Research: Atmospheres **122**, 9391–9412 (2017) https://doi.org/10.1002/2017JD026546

[7] Sotiropoulou, G., Sullivan, S., Savre, J., Lloyd, G., Lachlan-Cope, T., Ekman, A.M.L., Nenes, A.: The impact of secondary ice production on arctic stratocumulus. Atmospheric Chemistry and Physics **20**(3), 1301–1316 (2020) https://doi.org/10.5194/acp-20-1301-2020

[8] Pruppacher, H.R., Klett, J.D., Wang, P.K.: Microphysics of clouds and precipitation. Taylor & Francis (1998)

[9] Chisnell, R.F., Latham, J.: Ice particle multiplication in cumulus clouds. Quarterly Journal of the Royal Meteorological Society **102**, 133–156 (1976) https://doi.org/10.1002/qj.49710243111

[10] Yano, J.I., Phillips, V.T.J.: Ice-ice collisions: An ice multiplication process in atmospheric clouds. Journal of the Atmospheric Sciences **68**, 322–333 (2011) https://doi.org/10.1175/2010JAS3607.1

[11] Phillips, V.T.J., Patade, S., Gutierrez, J., Bansemer, A.: Secondary ice production by fragmentation of freezing drops: Formulation and theory. Journal of the Atmospheric Sciences **75**, 3031–3070 (2018) https://doi.org/10.1175/JAS-D-17-0190.1

[12] Phillips, V.T.J.: Ice multiplication by fragmentation during quasi-spherical freezing of raindrops: A theoretical investigation. J. Atmos. Sci. **78**(10), 3215–3228 (2021) https://doi.org/10.1175/JAS-D-20-0309.1

[13] Phillips, V.T.J., *et al.*: Multiple environmental influences on the lightning of cold-based continental cumulonimbus clouds. part i: Description and validation of model. Journal of the Atmospheric Sciences **77**, 3999–4024 (2020) https://doi.org/10.1175/JAS-D-19-0200.1

[14] Phillips, V.T.J., Patade, S.: Multiple environmental influences on the lightning of cold-based continental convection. part ii: Sensitivity tests for its charge structure and land–ocean contrast. Journal of the Atmospheric Sciences **79**, 263–300 (2022) https://doi.org/10.1175/JAS-D-20-0234.1

[15] Latham, J., Dye, J.E.: Calculations on the electrical development of a small thunderstorm. Journal of Geophysical Research **94**, 13141–13144 (1989) https://doi.org/10.1029/JD094iD11p13141

[16] Saunders, C.P.R., Keith, W.D., Mitzeva, R.P.: The effect of liquid water on thunderstorm charging. Journal of Geophysical Research **96**, 11007–11017 (1991) https://doi.org/10.1029/91JD00970

[17] Helsdon, J.H., Gattaleeradapan, S., Farley, R.D., Waits, C.: An examination of the convective charging hypothesis: Charge structure, electric fields, and maxwell currents. Journal of Geophysical Research **107**, 4630 (2002) https://doi.org/10.1029/2001JD001495

[18] Mansell, E.R., Ziegler, C.L., Bruning, E.R.: Simulated electrification of a small thunderstorm with two-moment bulk microphysics. Journal of the Atmospheric Sciences **67**, 171–194 (2010) https://doi.org/10.1175/2009JAS2965.1

[19] Waman, D., Patade, S., Jadav, A., Deshmukh, A., Gupta, A.K., Phillips, V.T.J., Bansemer, A., DeMott, P.J.: Dependencies of four mechanisms of secondary ice production on cloud-top temperature in a continental convective storm. Journal of the Atmospheric Sciences **79**, 3375–3404 (2022) https://doi.org/10.1175/JAS-D-21-0278.1

[20] Waman, D., Deshmukh, A., Jadav, A., Patade, S., Gautam, M., Phillips, V.T.J., Bansemer, A., Jakobsson, J.: Effects from time dependence of ice nucleus activity for contrasting cloud types. Journal of the Atmospheric Sciences **80**, 2013–2039 (2023)

[21] Seidel, J.S., Kiselev, A.A., Keinert, A., Stratmann, F., Leisner, T., Hartmann, S.: Secondary ice production–no evidence of efficient rime-splintering mechanism. Atmospheric Chemistry and Physics **24**(9), 5247–5263 (2024)

[22] Deshmukh, A., Phillips, V.T.J., Bansemer, A., Patade, S., Waman, D.: New empirical formulation for the sublimational breakup of graupel and dendritic snow. Journal of the Atmospheric Sciences **79**, 317–336 (2022) https://doi.org/10.1175/JAS-D-20-0275.1

[23] James, R.L., Phillips, V.T.J., Connolly, P.J.: Secondary ice production during the break-up of freezing water drops on impact with ice particles. Atmospheric Chemistry and Physics **21**(24), 18519–18530 (2021) https://doi.org/10.5194/acp-21-18519-2021

[24] Phillips, V.T.J., Yano, J.I., Khain, A.: Ice multiplication by breakup in ice-ice collisions. part i: Theoretical formulation. Journal of the Atmospheric Sciences **74**, 1705–1719 (2017) https://doi.org/10.1175/JAS-D-16-0224.1

[25] Phillips, V.T.J., *et al.*: Ice multiplication by breakup in ice-ice collisions. part ii: Numerical simulations. Journal of the Atmospheric Sciences **74**, 2789–2811 (2017) https://doi.org/10.1175/JAS-D-16-0223.1

[26] Phillips, V.T.J., *et al.*: Potential impacts from biological aerosols on ensembles of continental clouds simulated numerically. Biogeosciences **6**, 987–1014 (2009) https://doi.org/10.5194/BG-6-987-2009

[27] Skamarock, W.C., Klemp, J.B., Dudhia, J., Gill, D.O., Barker, D.M., Wang, W., Powers, J.G.: A description of the advanced research wrf version 2. Technical Report NCAR/TN-468+STR, National Center for Atmospheric Research (2005)

[28] Phillips, V.T.J., Donner, L.J., Garner, S.T.: Nucleation processes in deep convection simulated by a cloud-system-resolving model with double-moment bulk microphysics. Journal of the Atmospheric Sciences **64**, 738–761 (2007) https://doi.org/10.1175/JAS3869.1

[29] Phillips, V.T.J., DeMott, P.J., Andronache, C., Pratt, K.A., Prather, K.A., Subramanian, R., Twohy, C.: Improvements to an empirical parameterization of heterogeneous ice nucleation and its comparison with observations. Journal of the Atmospheric Sciences **70**, 378–409 (2013) https://doi.org/10.1175/JAS-D-12-080.1

[30] Phillips, V.T.J., Formenton, M., Bansemer, A., Kudzotsa, I., Lienert, B.: A parameterization of sticking efficiency for collisions of snow and graupel with ice crystals: Theory and comparison with observations. Journal of the Atmospheric Sciences **72**, 4885–4902 (2015) https://doi.org/10.1175/JAS-D-14-0096.1

[31] Barthe, C., Molinie, G., Pinty, J.-P.: Description and first results of an explicit electrical scheme in a 3d cloud resolving model. Atmospheric Research **76**, 95–113 (2005) https://doi.org/10.1016/j.atmosres.2004.11.021

[32] Takahashi, T.: Riming electrification as a charge generation mechanism in thunderstorms. Journal of the Atmospheric Sciences **35**, 1536–1548 (1978) https://doi.org/10.1175/1520-0469(1978)035⟨1536:REAACG⟩2.0.CO;2

[33] Takahashi, T.: Thunderstorm electrification—a numerical study. Journal of the Atmospheric Sciences **41**, 2541–2558 (1984) https://doi.org/10.1175/1520-0469(1984)041⟨2541:TENS⟩2.0.CO;2

[34] Heymsfield, A.J., et al.: Extinction-ice water content-effective radius algorithms for calipso. Geophysical Research Letters **32**(10) (2005) https://doi.org/10.1029/2005GL022742

Supplementary Files

This is a list of supplementary files associated with this preprint. Click to download.

- SIPPartIIsppl.pdf